

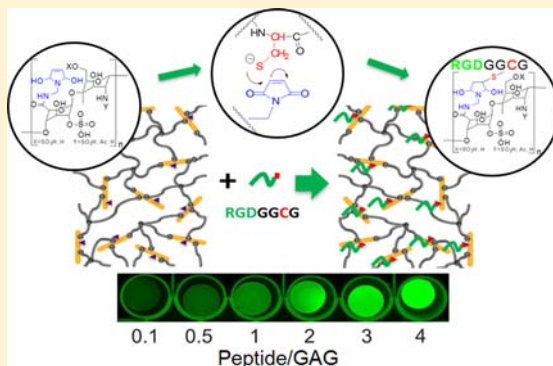
# Chemoselective Peptide Functionalization of starPEG-GAG Hydrogels

Mikhail V. Tsurkan,<sup>†</sup> Karolina Chwalek,<sup>†</sup> Melanie Schoder, Uwe Freudenberg, and Carsten Werner\*

Leibniz-Institut für Polymerforschung Dresden e.V., Max Bergmann Center of Biomaterials Dresden, Hohe Str. 6, 01069 Dresden, Germany

Technische Universität Dresden, Center for Regenerative Therapies Dresden, Fetscherstr. 105, 01307 Dresden, Germany

**ABSTRACT:** Glycosaminoglycan (GAG)-based hydrogels gain increasing interest in regenerative therapies. To support specific applications, the biomolecular functionality of gel matrices needs to be customized via conjugation of peptide sequences that mediate cell adhesion, expansion and differentiation. Herein, we present an orthogonal strategy for the formation and chemoselective functionalization of starPEG-GAG hydrogels, utilizing the uniform and specific conjugation of peptides and GAGs for customizing the resulting materials. The introduced approach was applied for the incorporation of three different types of RGD peptides to analyze the influence of peptide sequence and conformation on adhesion and morphogenesis of endothelial cells (ECs) grown on the peptide-containing starPEG-GAG hydrogels. The strongest cellular response was observed for hydrogels functionalized with cycloRGD followed by linear forms of RGDSP and RGD, showing that morphogenesis and growth rate of ECs is controlled by both type and quantity of the conjugated peptides.



## INTRODUCTION

Biohybrid materials containing glycosaminoglycans (GAGs) and synthetic polymers have attracted growing attention over the past decade<sup>1,2</sup> due to their unique capability of complexing a plethora of cell instructive signaling molecules<sup>3</sup> and their tissue-like physicochemical characteristics.<sup>4</sup> However, orthogonal conjugation techniques are required for independent cross-linking of polymeric precursors and implementing bioactive moieties to customize the resulting materials.<sup>5</sup>

GAGs are native polysaccharides found in the extracellular matrix (ECM) where they provide mechanical (hyaluronan, chondroitin, and others) and regulatory functions by binding, storage, and release of growth factors (heparan sulfate and heparin). Several recent reports concerned studies to combine GAGs with a synthetic polymer such as poly(ethylene glycol) (PEG) into binary polymer networks.<sup>6–8</sup> In general, plain GAG-based materials poorly support anchorage-dependent cells and, therefore, require additional functionalization with cell binding peptides.<sup>9</sup> A variety of peptide sequences (RGD, SIKVAV, YIGSR, GFOGER) derived from ECM proteins (collagen, fibronectin, vitronectin, laminin) has been demonstrated to enable cell adhesion, proliferation, and differentiation within synthetic materials.<sup>10</sup> Among them, RGD, the minimal integrin binding sequence, is most widely used to control cell attachment.<sup>10–12</sup> The recognition of the RGD sequence by multiple integrin receptors depends on flanking residues (X)RGD(X) as well as its three-dimensional structure which together modulate the integrin binding.<sup>13</sup> In the native state, the RGD sequence has a looped conformation which binds preferentially to  $\alpha_v\beta_3$  integrin, while the linear conformation is more selective to  $\alpha_5\beta_1$  integrin.<sup>5,14</sup> Hence, the different RGD

isoforms may initiate different signaling pathways and subsequently result in a different cell response.<sup>9</sup> Thus, they can be potentially utilized in biomaterial applications to manipulate the specificity and strength of cell adhesion on engineered substrates for directing the cell fate exogenously. As the differing structure of linear and cyclic RGD may result in a different turnover rate with GAGs during conjugation reactions producing a set of comparable GAG gels with different peptides requires a far-reaching level of control over the utilized chemistry.

GAGs consist of repeated disaccharide sequences with a characteristic degree of sulfation. Besides keratin sulfate, all GAGs contain carboxylic group which are commonly used for reactive conjugation. Thus, GAG cross-linking and functionalization are mainly performed with carbodiimide chemistry which today is the chemistry of choice for producing GAG containing biomaterials.<sup>6,15,16</sup> Several synthetic strategies such as blending<sup>6,15</sup> or postpolymerization<sup>17–19</sup> via carbodiimide chemistry were recently developed to immobilize the peptides in GAG-containing hydrogels. However, in carbodiimide chemistry unprotected functional groups of peptides can undergo intramolecular and intermolecular side reactions which affect the amount, distribution, and bioactivity of the immobilized peptides. Therefore, chemoselective approaches offering better selectivity and reactivity of bioactive peptides with GAG-containing hydrogel materials are needed. Functionalization reactions should be fast and applicable at low

**Received:** May 15, 2014

**Revised:** September 15, 2014

**Published:** September 17, 2014

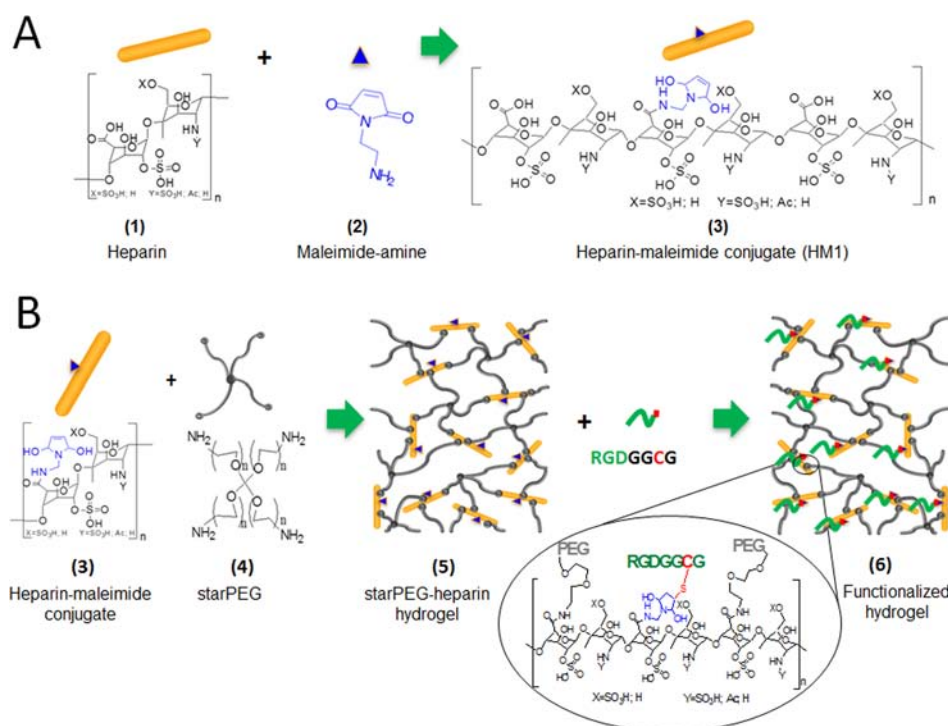


**Figure 1.** Synthesis and chemoselective peptide conjugation of starPEG-heparin hydrogels. (A) Synthetic scheme of heparin–maleimide conjugate formation. (B) Synthetic scheme of starPEG-heparin hydrogel formation followed by the chemoselective functionalization of the resulting hydrogel material with a bioactive peptide.

concentrations of reagents. It should provide a high selectivity in the presence of common functional groups to ensure oriented and homogeneous peptide immobilization without affecting materials properties such as stiffness or swelling. Meeting all these criteria, Michael-type addition reaction can selectively link a thiol group (cysteine residue) of any peptide with an electronically deficient double bond of maleimide or acrylic groups in a polymer backbone by creating a stable thioether bond. We have utilized this reaction to show a novel orthogonal approach for the functionalization of a modular set of starPEG-heparin hydrogels (Figure 1).<sup>17</sup> The proposed method enables the quantitative and uniform attachment of various biofunctional peptides without affecting the hydrogel network, thereby preserving the intrinsic mechanical properties of the material. To illustrate the advantages of the introduced approach, we furthermore studied the response of human endothelial cells (ECs) to three different forms of RGD-ligands immobilized within starPEG-heparin hydrogels. ECs change the morphology from a cobblestone-like to a spindle-shaped phenotype and form networks of loosely associated cellular structures in vitro before undergoing vascular tube formation.<sup>20</sup> While the protocols described in this report were optimized for starPEG-heparin hydrogels, the introduced method is considered to be similarly applicable for hydrogels or surfaces containing other natural (GAGs, alginates) and synthetic (dextran carboxyl, carboxymethyl cellulose) polymer components with available carboxyl groups.

## RESULTS AND DISCUSSION

**Material Design.** The main goal of this study was development of a synthetic pathway for the functionalization of GAG-containing hydrogel materials with a precise amount of bioactive peptides. In our synthetic design (Figure 1), heparin (1) is first functionalized with a known amount of *N*-(2-

aminoethyl)maleimide (2) using EDC/sNHS chemistry (Figure 1A). The stoichiometric ratio of heparin and maleimide in this step determines the heparin/maleimide ratio in the resulting conjugate (3). The purified heparin–maleimide conjugate is activated once more by EDC/sNHS for the subsequent reaction with amino-terminated starPEG (4) resulting in a starPEG-heparin hydrogel network with evenly distributed maleimide groups (5) (Figure 1B). In the final step, the maleimide groups of the hydrogel selectively react with the thiol group of cysteine of RGD-containing peptides producing a hydrogel material with evenly distributed RGD decoration (6). The high reactivity of thiols in Michael addition reaction guarantees their quantitative conversion, allowing for the precise adjustment of the concentration of the immobilized peptide by the amount of either the applied peptide or the available maleimide groups, respectively. Hence, the heparin/maleimide ratio of the conjugate can be used to define the peptide functionalization of the hydrogel. The explored synthetic strategy can be readily applied to various carbodiimide chemistry protocols for the formation of an array of customized, GAG-based materials.

**Formation of Heparin–Maleimide Conjugates.** The formation of heparin–maleimide conjugates via carbodiimide chemistry was first described by Küick and co-workers.<sup>21</sup> In that report, two different methods using EDC/*N*-hydroxy succinimide (NHS) or EDC/1-hydroxybenzotriazol (HOBt) were found to be efficient for the covalent coupling of maleimide amine and heparin. EDC/HOBt was proposed as a better reagent for the formation of the conjugates due to a higher yield and the absence of side reactions such as ring opening aminolysis of the maleimide amine. Here, we propose an alternative technique based on EDC/sNHS chemistry which allows for the attachment of a defined number of fully reactive maleimide groups to the backbone of GAG molecules such as

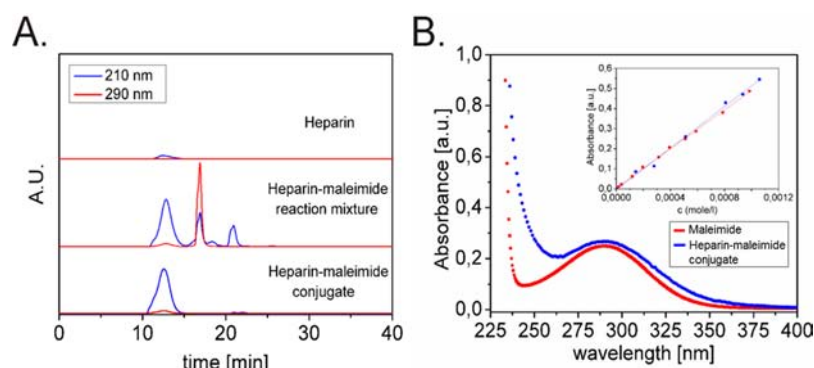


**Figure 2.** Characterization of heparin–maleimide conjugates. (A) High performance size exclusion chromatograms of heparin, the reaction mixture of heparin with *N*-(2-aminoethyl)maleimide (1:4) and the purified heparin–maleimide conjugate (210 nm absorbance reflects heparin, 290 nm absorbance the maleimide group, respectively). (B) UV–vis spectra of *N*-(2-aminoethyl)maleimide trifluoroacetic salt (red) and the heparin–maleimide conjugate (blue) in water; the inset highlights the changes of absorbance at 290 nm vs the concentration of the maleimide moieties in *N*-(2-aminoethyl)maleimide trifluoroacetic salt (red) and in heparin–maleimide conjugate (blue).

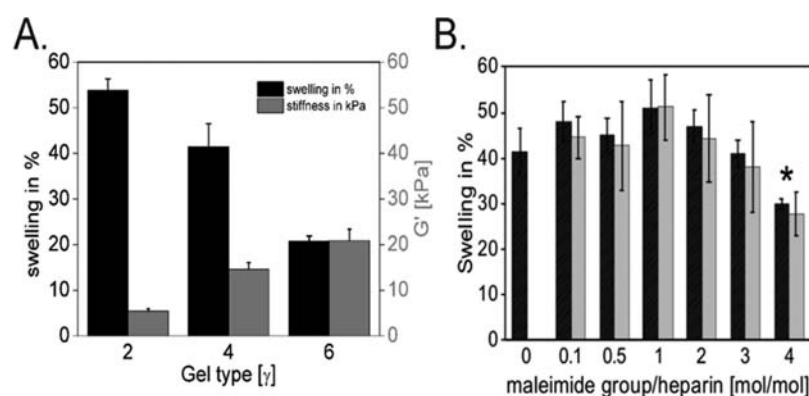


**Figure 3.** Physical properties of the starPEG-heparin hydrogels containing heparin–maleimide conjugates. (A) Rheology data showing the influence of the molar ratio of the building blocks  $\gamma$  (proportional to the cross-linking degree) on the stiffness (right scale) and swelling degree (left scale). (B) Swelling degree vs the amount of maleimide groups per heparin molecule before (black bars) and after (gray bars) the peptide conjugation.

heparin.<sup>22</sup> The high solubility of sNHS in aqueous solutions allowed us to perform the reaction in a very concentrated solution of heparin (10% solid content), which resulted in high efficiency (>95%) of the conjugate formation. NMR was previously used to analyze the products,<sup>21</sup> while we utilized here high performance size exclusion chromatography (HPSEC) as a more sensitive technique that allows for the fast separation of the GAGs from any low molecular weight species such as the unreacted maleimide amine (Figure 2A). Maleimide has a characteristic absorbance at 290 nm and the absence of any absorbance of GAGs in this region allows us to follow the reaction by HPSEC and UV–vis quantification.

In the HPSEC analysis, heparin elutes as a single wide peak at 13 min with a weak absorbance at 210 nm. For the reaction mixture, peaks at 13, 17, and 22 min elution time were detected. The peak at 17 min corresponds to sNHS and the product of the hydrolysis of EDC, and the small peak at 22 min reflects the unreacted maleimide (weak absorbance in the 290 nm channel). The peak at 13 min has a similar elution time as the unmodified heparin, but absorbs at both 210 and 290 nm. The chromatogram of the dialyzed reaction mixture revealed the presence of only one peak with an elution time of 13 min and a significant absorbance at both 210 and 290 nm which corresponds to the conjugate (290 nm absorbance is characteristics for the maleimide group). The integration of the absorbance peak at 290 nm in the HPSEC chromatogram of

the reaction mixture showed that about 95–98% of the maleimide amine is reacted. Thus, the use of 5% excess of the maleimide amine leads to the formation of a conjugate with the chosen heparin/maleimide ratio which can be determined by the UV–vis absorbance (Figure 2B). The UV–vis spectrum of the maleimide amine in water is similar in both shape and intensity to the spectrum of the heparin–maleimide conjugate containing similar amounts of maleimide (measured at the same conditions) (Figure 2B). The maleimide amine has a weak absorbance at 250–350 nm with a broad maximum at 280–300 nm, and its extinction coefficient at 290 nm was determined to be  $490 \text{ L mol}^{-1} \text{ cm}^{-1}$  ( $\pm 3\%$ ) (Figure 2B inset). The plot of absorbance vs theoretical concentration of maleimide groups in the conjugate showed a linear increase of the absorbance with the increasing amount of immobilized maleimide moieties and nearly meets the plot of the pure maleimide amine. The extinction coefficient of the maleimide conjugated to heparin is measured as  $510 \text{ L mol}^{-1} \text{ cm}^{-1}$  ( $\pm 6\%$ ) which coincides within experimental error with that of free maleimide amide. Thus, the concentration of the heparin–maleimide conjugates can be easily determined by spectroscopic measurements. Importantly, the absorbance of the maleimide group at 250–350 nm corresponds to its conjugated  $\pi$ -system and the loss of this conjugation by hydrolysis or Michael addition reaction leads to the loss of this absorbance. Therefore, the described method exclusively determines



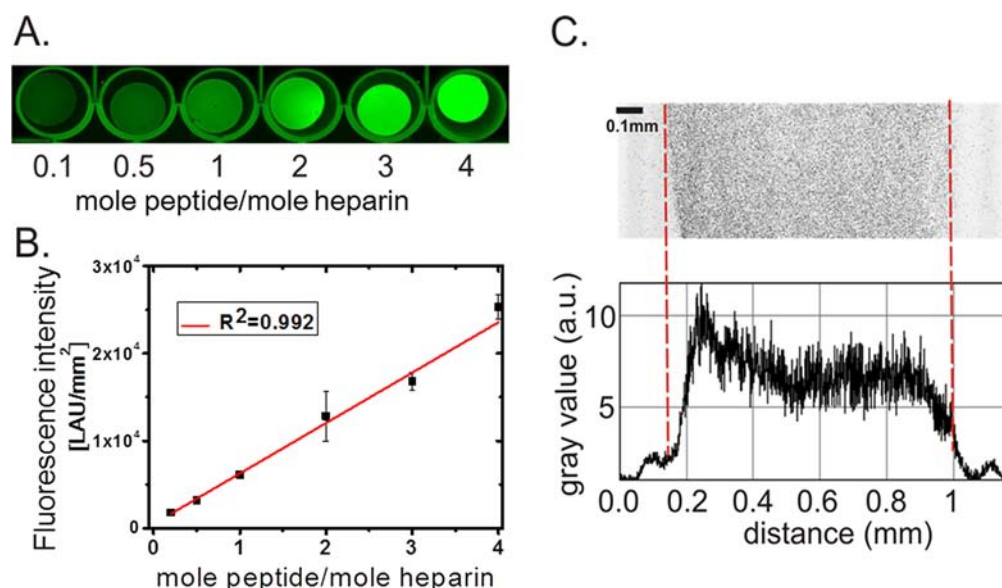


**Figure 4.** Conjugation of fluorescently labeled RGD peptide to the hydrogels. (A) Fluorescence image of hydrogels functionalized with gradually increasing concentrations of fluorescent ATTO-RGD peptide conjugate. (B) Quantification of the fluorescence intensity from the images of hydrogels containing gradually increasing amounts of fluorescent ATTO-RGD peptide conjugate. (C) Cross-sectional image of the hydrogel functionalized with fluorescent ATTO-RGD conjugate and histogram of fluorescence intensity through the gel showing a homogeneous peptide distribution throughout the hydrogel.

maleimide groups that can be converted in the Michael addition reaction and is not influenced by any side products of the synthesis (resulting from maleimide hydrolysis or intermolecular aminolysis).

**Hydrogel Formation and Characterization.** Carbodiimide chemistry is widely used for the formation of GAG containing hydrogel materials. Herein, we refer to a modular starPEG-heparin hydrogel platform which allows for the independent variation of biomolecular composition and physical network properties.<sup>17</sup> In this approach, the carboxylic groups of heparin (average molecular weight of 14 kDa, with approximately 22–24 carboxylic groups per molecule) and terminating amino groups of starPEG (average molecular weight of 10 kDa) are cross-linked after EDC/sNHS carbodiimide activation of the carboxylic groups. Applying different starPEG/heparin ratios ( $\gamma$  = molar ratio starPEG/heparin)<sup>23</sup> while keeping the total mass of the reagents constant (11% total solid content) allows for the formation of hydrogel materials with defined variations in stiffness and swelling degree (Figure 3A). As theoretically predicted and experimentally confirmed, a constant concentration of heparin ( $\sim 11$  mg/mL which is  $7.86 \times 10^{-4}$  mol/L) can be obtained for a wide range of stiffness and swelling degrees of the swollen materials.<sup>17</sup> Thus, the substitution of heparin with heparin–maleimide conjugates during hydrogel formation leads to a defined concentration of maleimide groups that is independent of the physical characteristics of the hydrogel material.

The swelling degree was evaluated for a series of hydrogels with increasing concentration of maleimide groups (Figure 3B), confirming that the incorporation of conjugates with up to three maleimide groups per heparin molecule did not affect the swelling significantly. Further increase of the heparin conjugation resulted in decreased swelling ( $>30\%$ ) which may be caused by additional bonds formed between the maleimide groups and  $-\text{NH}_2$  groups of PEG molecules during hydrogel formation and/or the altered characteristics of the modified heparin with respect to excluded volume forces. The reactivity

of chemical groups in Michael addition reactions drops dramatically in the following sequence: sulfhydryls  $>$  secondary amines  $>$  primary amines, with primary amines reacting over extended time and under harsh conditions only.<sup>24,25</sup> Heparin–maleimide conjugates mixed with  $\text{NH}_2$ -terminated starPEG did not form a hydrogel, even after several days of incubation, which suggests that this side reaction is of minor importance. The solubility of heparin–maleimide conjugates in aqueous solutions decreases with increasing amounts of maleimide groups. While the mono- and disubstituted heparin conjugates dissolved instantly in PBS, heparin conjugates with six and more maleimide groups required several minutes of ultrasound treatment. Therefore, the observed decrease in swelling is mainly attributed to the hydrophobic character of the maleimide groups and consequently altered excluded volume forces acting within the hydrogel. This finding points at the potential impact of the maleimide conjugation of the GAG on the mechanical properties of the hydrogel materials formed thereof. This effect is expected to be even more pronounced for GAGs with lower sulfation degree such as hyaluronan or chondroitin.

**Quantification of Peptide Functionality.** In aqueous environments the imido group of maleimides slowly undergoes ring opening hydrolysis into maleamic acid derivatives.<sup>26</sup> Thus, the activity of maleimide groups conjugated to heparin was evaluated after hydrogel formation with a fluorescently labeled RGD (RGD-(ATTO-460)) peptide. It is important to notice that due to self-quenching effects only 10% of the applied peptide was labeled. The application of 100% labeled peptide lead to self-quenching of the fluorescent label<sup>27</sup> which resulted in fluorescence bleaching at higher degrees of the peptide functionalization of the gels. An excess of the peptide solution ( $\text{pH} > 7$ ) was applied to a series of hydrogels with different amounts of heparin coupled maleimide groups after the fluorescence intensity was measured (Figure 4). The gradually increasing fluorescence intensity of the hydrogel samples (Figure 4A) is indicative of the successful reaction between

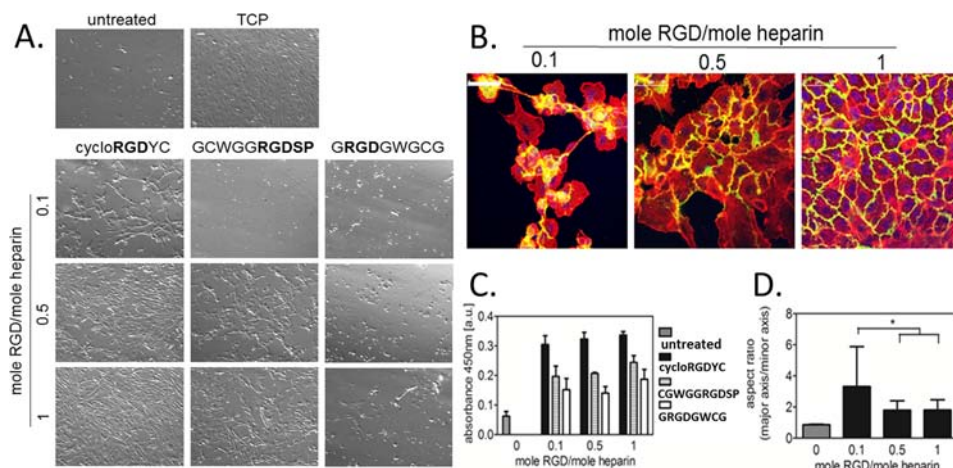


**Figure 5.** Endothelial cells growing on starPEG-heparin hydrogels functionalized with different types and concentrations of RGD peptides (cycloRGDYC, GCWGGRGDSP, and GRGDGWGCG) at 7 days of culture. (A) Light microscopy images of cells. Scale bar 50  $\mu$ m. TCP refers to tissue culture plastic. (B) Confocal images (green, CD31; red, actin; blue, DAPI). Scale bar 50  $\mu$ m. (C) WST-1 assay representing EC viability on RGD-decorated hydrogels. (D) Quantification of EC morphology on cRGD functionalized hydrogels.

the maleimide groups and the RGD-(ATTO-460) peptide proving that the maleimide groups remained reactive after hydrogel formation. The quantification of the fluorescence intensities revealed their linear dependency on the amount of the (fluorescence-labeled) peptide conjugated to the maleimide groups (Figure 4B). Together, these results showed that the peptide conjugation to the maleimide group is quantitative and can be successfully utilized for the customization of the hydrogel materials. The amount of immobilized peptides can be controlled by both the concentration of maleimide groups in the hydrogel and the amount of the applied peptide. The application of a constant maleimide amount within the hydrogel combined with the variation of the applied amount of peptide could be advantageous for practical reasons, as it would circumvent the necessity of preparing multiple heparin–maleimide conjugates. The peptide distribution throughout the hydrogel was visualized with confocal microscopy (Figure 4C) showing homogeneous fluorescence intensity corresponding to the uniform peptide distribution. Together, these results show that the concentration of the immobilized peptide can be precisely adjusted by the amount of either the applied peptide or the available maleimide groups, respectively.

**Cell Adhesion and Viability.** Density and integrin binding constant of immobilized ligand motifs determine the cell adhesiveness of functionalized biomaterial. The precise control over concentration and orientation of the conjugated peptides in the developed set of hydrogel materials allows for direct comparison of the efficacy of different peptide ligands. This was demonstrated for expansion and morphogenesis of human umbilical vein endothelial cells (HUVECs) exposed to three types of immobilized RGD peptides: cycloRGDYC, GCWGGRGDSP, and GRGDGWGCG (Figure 5) which vary in their flanking residues (X)RGD(X) as well as in their three-dimensional structures which together modulate the integrin binding.

Hydrogels of constant stiffness ( $G' \approx 6$  kPa) and maleimide content (1 and 2 mol maleimide per mol heparin) were functionalized with various amounts of each peptide: 0.1, 0.5, and 1 mol peptide/mol heparin, which correspond to peptide concentrations of  $7.86 \times 10^{-5}$  mol/L;  $3.93 \times 10^{-4}$  mol/L, and  $7.86 \times 10^{-4}$  mol/L. To demonstrate the specificity of the peptide-mediated cell attachment, peptide-free hydrogels were

used as a control. As anticipated, due to the nonadhesive behavior of PEG<sup>28</sup> no cell adhesion was detected on this sample; cell attachment and spreading were observed only when the hydrogel supports were functionalized with the adhesive ligands (Figure 5A).

The amount of immobilized peptide determined the degree of cellular attachment within the range of 0.1 to 1 mol RGD/mol heparin, while no difference between the materials with 1 and 2 mol RGD/mol heparin was observed. The efficacy of cell attachment was also found to depend on the particular type of RGD peptide with increasing cell adhesion in the series cycloRGDYC > GCWGGRGDSP > GRGDGWGCG. CycloRGDYC, as the most effective peptide, resulted in a confluent cell layer at 1 mol RGD/mol heparin, whereas lower concentrations led to the formation of a network of cord-like structures (Figure 5A and B). In the case of the GCWGGRGDSP peptide higher concentrations were required (0.5 vs 0.1 mol RGD/mol heparin) to obtain a similar cell response. GRGDGWGCG peptide modified hydrogels were poorly colonized with cells. However, even in this case the attached cells were—in contrast to cells on the peptide-free hydrogel—evenly spread, indicating a peptide mediated cell adhesion, which is in line with earlier reports on cell attachment being mediated by weakly binding RGD conformations at elevated surface concentrations.<sup>29</sup> Moreover, the adhesion ligand density was demonstrated to regulate the clustering of integrin receptors and, thus, adhesion mediated signaling events, ultimately determining cell fate.<sup>5,30</sup> A colorimetric cell viability assay confirmed the microscopic observations, additionally showing that EC density after 7 days is much higher on cycloRGDYC when compared to GCWGGRGDSP, which itself is more efficient than GRGDGWGCG (Figure 5C). Comparable results have been reported for several anchorage dependent cell types by Hirano et al., who showed that adding serine following the RGD motif increases cell adhesion.<sup>31</sup> It suggests that the difference in the type of amino acids flanking the RGD motif in our two linear RGD peptides influences the recognition by cellular receptors. Moreover, in agreement with our findings, cyclization of the linear RGD peptide was reported to constrain its conformation, increase the peptide affinity for the  $\alpha v \beta 3$  integrin,<sup>32</sup> and thus results in increased cell attachment.<sup>14,33</sup>

**Cell Morphology.** ECs sense their microenvironment with respect to type and quantity of adhesion ligands and respond with morphology changes. Fluorescence microscopy revealed a correlation between the EC morphology and the concentration of immobilized RGD peptides (Figure 5C). Hydrogel functionalization with a low concentration of cycloRGDYC (0.1 mol RGD/mol heparin) resulted in EC elongation and morphogenesis as indicated by a significantly higher cell shape aspect ratio (ratio of major to minor axis of the cells) (Figure 5A,B,D). In contrast, higher concentrations of cycloRGDYC resulted in a spread EC morphology and the formation of confluent layers. Thus, while cell adhesion and expansion increased with the amount of incorporated peptide, EC morphogenesis was most prominent at low or intermediate peptide concentrations which confirms earlier reports by us<sup>23,34</sup> and others.<sup>35,36</sup> Moreover, type and quantity of adhesion sites affect cell migration<sup>37</sup> and vascular morphogenesis because EC elongation requires a sufficient number of attachment points that physically resist cell-generated tensile forces.<sup>35</sup> Folkman and Ingber showed that ECs retract and form branching networks with hollow tubular structures only when cultured on a substrate of moderate ligand density,<sup>35,38</sup> which is in line with our results.

## CONCLUSIONS

A chemoselective strategy for conjugating adhesion receptor ligands to the GAG components of biohybrid hydrogel materials was established. The discovered inactivity effect of maleimide groups during the formation of starPEG-heparin hydrogels enables a new orthogonal strategy for the application of Michael-type addition reactions. While the direct carbodiimide chemistry is still widely applied for nonchemoselective peptide functionalization,<sup>15–17,40–42</sup> the proposed method allows for the precise control over the concentration of the integrated bioactive peptides without affecting the intrinsic physical network properties. Materials functionalized with different types of RGD peptides in different concentrations were successfully utilized for elucidating their impact on the modulation of EC attachment and morphogenesis, crucial events in the induction of angiogenesis. Beyond that, the presented strategy is considered a powerful general means for customizing GAG based matrices by covalently attached bioactive species in precisely defined amounts.

## EXPERIMENTAL PROCEDURES

**Reagents and Supplies.** All solvents and reagents for peptide synthesis and purification were purchased from IRIS Biotech GmbH (Marktredwitz, Germany). 1-ethyl-3-(3-(dimethylamino)propyl)carbodiimide (EDC), *N*-hydroxysulfosuccinimide sodium salt (sNHS), *N*-(2-aminoethyl)maleimide trifluoroacetate salt, and tris(2-carboxyethyl)phosphine (TCEP) were purchased from Sigma-Aldrich (St. Louis, USA). Heparin (Mw = 14 000) was purchased from Merck (Darmstadt, Germany). Four-armed amine terminated polyethylene glycol (starPEG) (Mn = 10.0 × 10<sup>3</sup>; PDI = 1.09) was purchased from Polymer Source (Montreal, Canada). All reagents were used without purification.

**Peptide Syntheses and Purification.** All peptides were synthesized by solid-phase methods using an Activo P11 (Activotec, Cambridge, UK) peptide synthesizer and standard Fmoc-chemistry. Specifically, the 0.3 mmol scale protocol with a C-terminal capping protection strategy by amide was used.

Amino acid activation was achieved by *O*-(benzotriazol-1-yl)-*N,N,N',N'*-tetramethyluronium tetrafluoroborate (TBTU), and 1-hydroxybenzotriazole (HOBt) in DMF with diisopropylethylamine (DIPEA) as a base. Deprotection of the amino acid side chains and cleavage from the resin was performed by reaction with a mixture of trifluoroacetic acid (TFA) (87.5% v/v), phenol (5% v/v), tri-isopropyl silane (TIPS) (2.5% v/v), and water (5% v/v) for 2.5 h at room temperature. The crude peptides were then precipitated in cold anhydrous diethyl ether, collected by vacuum filtration, and dried under vacuum. Final purification was achieved by preparative reversed-phase high performance liquid chromatography (HPLC) on a preparative reversed-phase XBridge Prep C-18 column (10 μm particle size, 19 × 250 mm; Waters, Milford, USA). A linear gradient of water/acetonitrile containing 0.1% (v/v) TFA was used as the mobile phase. The HPLC separation runs were performed on a two-pump system (1200 Series; Agilent Technologies, Santa Clara, USA) equipped with an UV/vis diode array detector/spectrophotometer. The collected peptides were lyophilized, and their purity was verified by analytical HPLC and electrospray ionization mass spectrometry. All ESI-MS measurements were performed on a Waters TQ Detector ACQUITYuplc mass spectrometer (Waters, Milford, USA).

**Chromatography Analysis.** All chromatography was performed on a two-pump system (1100 Series; Agilent Technologies, Santa Clara, USA) equipped with a UV/vis detector/spectrophotometer and a 1 cm path length cell was used. The monitoring wavelengths were set to a wavelength range of 210–300 nm. HPLC experiments were performed by analytical HPLC XBridge BEH 300 C-18 column (5 μm particle size, 2.1 × 250 mm; Waters, Milford, USA) over 40 min using the flow rate of 0.5 mL/min for the analytical column. A linear gradient of water/acetonitrile containing 0.1% (v/v) TFA was used as the mobile phase. HPSEC experiments were performed on a BioSep-SEC-S 2000 column (Phenomenex, Torrance, USA). The peptide samples were eluted using standard phosphate buffered saline (PBS, pH 7.4), with 0.5 mL/min flow rate.

**Synthesis and Purification of Heparin–Maleimide Conjugates.** All the heparin–maleimide conjugates were formed using the same protocol. The amount of maleimide in the formed heparin–maleimide conjugate heparin was controlled by the ratio between heparin and *N*-(2-aminoethyl)-maleimide trifluoroacetate salt (limiting reagent) added to the reaction mixture. Threefold molar excess of EDC and 1.5-fold molar excess of sNHS (referring to the maleimide amine) were added to a solution of 0.5 g of heparin dissolved in 3 mL of ultrapure H<sub>2</sub>O. The amount of maleimide amine (5% excess to the theoretical amount) was 9.55 mg for HM1, 19.1 mg for HM2, 28.65 for HM3, and 38.2 mg for HM4 conjugates which correspond to one, two, three, and four maleimide molecules per heparin. The reaction mixture was kept at 4 °C for 20 min. Next, *N*-(2-aminoethyl)maleimide trifluoroacetate salt was dissolved in ddH<sub>2</sub>O (at 5 °C) and added to the reaction mixture. The final volume of the reaction mixture must not exceed 5 mL. The reaction was run overnight at room temperature. The conjugate was purified by dialysis (membrane with 5000–8000 molecular weight cutoff) against 800 mL of 1 M sodium chloride three times for 1 h in order to remove any unreacted maleimide amine. This was followed by dialysis against 800 mL of water at least four times for 1 h each. The product was then freeze-dried for at least 24 h and stored at –20 °C. Small aliquots were analyzed by UV–vis spectroscopy.



**UV-vis Spectroscopy.** All UV-vis spectra were measured on a single beam spectrophotometer (DU 800 Beckman Coulter, GmbH, Krefeld, Germany) using a 2 mm quartz cuvette (HELLMA optic GmbH, Jena, Germany).

**Hydrogel Formation.** The gels were prepared as previously described.<sup>17</sup> Briefly, a 2-fold excess of EDC and stoichiometric amounts of NHS were added to an aqueous solution of the heparin-maleimide conjugates dissolved in water. The reaction mixture was kept for 15 min at 4 °C in order to form heparin-NHS esters. Next, a stoichiometric amount of amine-terminated starPEG dissolved in water was added. The total volume of the reaction mixture was 1 mL and the total weight of heparin and starPEG mixture was about 110 mg (solid content 11%). The mixture polymerized in less than 1 h, and was kept overnight at room temperature for the completion of the reaction. The gel was swollen in water and then washed several times with PBS to remove the side products of the reaction and stored in PBS at 5 °C. Gels used for in vitro applications were prepared under sterile conditions and reagent solutions used in the preparation were sterilized by filtration through 0.2 µm filters (PVDF Acrodisc LC 13 mm, PALL Life Science, Port Washington, USA).

**Rheological Measurements.** Oscillating measurements on swollen gel disks (PBS) were carried out on a rotational rheometer (ARES LN2; TA Instruments, Eschborn, Germany), fitted with a parallel plate geometry (plate diameter = 25 mm) as described before.<sup>17</sup> Frequency sweeps were performed at 25 °C with a shear frequency range of  $10^{-1}$ – $10^2$  rad s<sup>-1</sup> and a strain amplitude of 2%. Mean values of the storage modulus were calculated. Experiments were performed in triplicate. The hydrogels were prepared as disks between Sigmacote (Sigma-Aldrich, München, Germany) coated coverslips of a defined diameter ( $D_i$  = 11 mm). The volumetric swelling of the gels was determined by the following equation:  $Q = (D_f/D_i)^3 V_{\text{react}}/V_0$ , where  $V_{\text{react}}$  is the volume of the cured reaction mixture and  $V_0$  is the volume of the dry gel ( $V_0 = n_{\text{PEG}} \cdot v_{\text{PEG}} + n_{\text{HEP}} \cdot v_{\text{HEP}}$ ;  $v_{\text{PEG}} = 8.006$  cm<sup>3</sup>/mol;  $v_{\text{HEP}} = 7.089$  cm<sup>3</sup>/mol),<sup>43</sup>  $D_i$  is the initial diameter of the nonswollen gel disk (after hydrogel formation), and  $D_f$  is the final diameter of the gel disk swollen for 24 h in PBS.

**Modification with RGD.** Upon polymerization, solid gels were immersed in a peptide solution in 100 mM borate buffer, pH 8, and incubated at 37 °C for 3 h. Subsequently, all samples were extensively washed with PBS (pH 7.4) to remove traces of unreacted peptide. Three peptide types were utilized in this study: cycloRGDYC, GCWGGRGDSP, and GRGDGWGCG. Moreover, a fluorescently labeled GRGDGWGCG (ATTO-GRGDGWGCG-CONH<sub>2</sub>) peptide was used for peptide quantification purpose.

**Fluorescent Quantification of Peptide Functionality.** Hydrogels were created as free loading discs of approximately 0.8 mm thickness and 11 mm in diameter. Fluorescently labeled RGD peptides (ATTO-GRGDGWGCG-CONH<sub>2</sub>) were immobilized to the hydrogel discs and imaged with a laser scanner (FujiFilm FLA-5100) at 473 nm wavelength. The intensity of the fluorescence was quantified with FujiFilm FLA-5100 software where the fluorescence signal is expressed as linear arbitrary unit across 1 mm<sup>2</sup> area (LAU/mm<sup>2</sup>). Additionally, hydrogels were scanned with a confocal microscope (Leica SP5) through the whole thickness of the disc (approximately 0.8 mm) and the fluorescent intensity of the z-projection was measured.

**Cell Culture Experiments.** Before cell seeding, hydrogels were equilibrated in cell culture medium for 1 h at 37 °C. Human umbilical vein endothelial cells (HUVECs), isolated according to the procedure proposed by Weis et al. were used.<sup>39</sup> The cells were cultured up to 80% confluence in ECGM medium (Promocell, Heidelberg, Germany) containing supplement at 37 °C and 5% CO<sub>2</sub>. Cells from passage 2–6 were used. Cell morphology, attachment and spreading were monitored daily with bright field microscope (Olympus IX50, 10x objective).

**Immunostaining.** At day 0 cells were seeded at a density of  $4 \times 10^4$ /cm<sup>2</sup> on following surfaces: nonfunctionalized hydrogels, hydrogels functionalized using 0.1, 0.5, or 1 mol RGD/mol heparin solution of cycloRGDYC, GCWGGRGDSP, or GRGDGWGCG peptides as specified above. The tissue culture plastic (TCP) was used as an additional control. Upon 7 days of culture the cells were washed with PBS and fixed with 4% paraformaldehyde (PFA) for 15 min at room temperature. Subsequently the cells were permeabilized with 0.2% Triton-X100 in PBS for 15 min and unspecific staining was blocked by 1 h incubation in blocking buffer (0.25% bovine serum albumin, 0.1% goat serum in PBS). Samples were stained with monoclonal mouse anti-CD31 (endothelial cell specific protein) (BD Bioscience, Heidelberg, Germany) and Alexa-Fluor 488 goat anti-mouse secondary (Invitrogen) antibodies. F-actin was visualized by Phalloidin CF633 (Biotum, Hayward, CA, USA). Confocal images were taken with a Leica SP5 microscope (Leica, Wetzlar, Germany), and ImageJ software (NIH) was used to quantify the aspect ratio of individual cells.<sup>23</sup> The aspect ratio was determined by calculating the ratio of the major axis of individual cells to their minor axis, with a higher aspect ratio indicating more elongated cells. Aspect ratios are recorded as means  $\pm$  standard deviation of >20.

**Viability/Proliferation WST-1 Assay.** At day 0 cells were seeded at a density of  $4 \times 10^4$ /cm<sup>2</sup>. After 7 days cell viability was estimated using a colorimetric WST-1 assay (Roche, Germany) according to the manufacturer's instructions. Briefly, cells were incubated for 30 min with WST-1 reagent diluted 1:10 (v:v) in serum-free ECGM medium, followed by a reading of the sample absorbance with plate reader (TECAN GENios) at 450 and 650 nm as the reference wavelength. The serum-free ECGM medium was used as a baseline control and its average absorbance value was subtracted from the value of the samples.

**Statistics.** Statistical analysis was performed with InStat software (GraphPad, CA, USA). Analysis of variance (ANOVA) was the primary analysis method using the Kruskal-Wallis test. Levels of significance were determined when \*  $p < 0.05$ , \*\*  $p < 0.01$ , \*\*\*  $p < 0.001$ .

## AUTHOR INFORMATION

### Corresponding Author

\*E-mail: werner@ipfdd.de. Tel. +49 (0)351 4658 531/Fax +49 (0)351 4658 533.

### Author Contributions

<sup>†</sup>Mikhail V. Tsurkan and Karolina Chwalek contributed equally.

### Notes

The authors declare no competing financial interest.

## ACKNOWLEDGMENTS

M.T., U.F., and C.W. were supported by the Deutsche Forschungsgemeinschaft (DFG) through grants SFB TR 67, WE 2539-7/1, SFB 655, and FOR/EXC999, and by the Leibniz

Association (SAW-2011-IPF-2 68). M.T. and C.W. were supported by the Seventh Framework Programme of the European Union through the Integrated Project ANGIO-SCAFF. C.W. was supported by the Bundesministerium für Bildung, Forschung, und Technologie (BMBF) through grant 01 GN 0946.

## REFERENCES

- (1) Li, Y., Rodrigues, J., and Tomas, H. (2012) Injectable and biodegradable hydrogels: gelation, biodegradation and biomedical applications. *Chem. Soc. Rev.* 41, 2193–221.
- (2) Seliktar, D. (2012) Designing cell-compatible hydrogels for biomedical applications. *Science* 336, 1124–1128.
- (3) Capila, I., and Linhardt, R. J. (2002) Heparin-protein interactions. *Angew. Chem., Int. Ed.* 41, 391–412.
- (4) Tessmar, J. K., and Gopferich, A. M. (2007) Customized PEG-derived copolymers for tissue-engineering applications. *Macromol. Biosci.* 7, 23–39.
- (5) Hersel, U., Dahmen, C., and Kessler, H. (2003) RGD modified polymers: biomaterials for stimulated cell adhesion and beyond. *Biomaterials* 24, 4385–4415.
- (6) Yamaguchi, N., and Kiick, K. L. (2005) Polysaccharide-poly(ethylene glycol) star copolymer as a scaffold for the production of bioactive hydrogels. *Biomacromolecules* 6, 1921–1930.
- (7) Cai, S., Liu, Y., Zheng Shu, X., and Prestwich, G. D. (2005) Injectable glycosaminoglycan hydrogels for controlled release of human basic fibroblast growth factor. *Biomaterials* 26, 6054–6067.
- (8) Burdick, J. A., and Prestwich, G. D. (2011) Hyaluronic acid hydrogels for biomedical applications. *Adv. Mater.* 23, H41–56.
- (9) Bellis, S. L. (2011) Advantages of RGD peptides for directing cell association with biomaterials. *Biomaterials* 32, 4205–4210.
- (10) Collier, J. H., and Segura, T. (2011) Evolving the use of peptides as components of biomaterials. *Biomaterials* 32, 4198–4204.
- (11) Yamada, K. M., and Kennedy, D. W. (1987) Peptide inhibitors of fibronectin, laminin, and other adhesion molecules: unique and shared features. *J. Cell Physiol.* 130, 21–28.
- (12) Hersel, U., Dahmen, C., and Kessler, H. (2003) RGD modified polymers: biomaterials for stimulated cell adhesion and beyond. *Biomaterials* 24, 4385–4415.
- (13) Pankov, R., and Yamada, K. M. (2002) Fibronectin at a glance. *J. Cell Sci.* 115, 3861–3863.
- (14) Xiao, Y., and Truskey, G. A. (1996) Effect of receptor-ligand affinity on the strength of endothelial cell adhesion. *Biophys. J.* 71, 2869–2884.
- (15) Kuo, J. W., Swann, D. A., and Prestwich, G. D. (1991) Chemical modification of hyaluronic acid by carbodiimides. *Bioconjugate Chem.* 2, 232–241.
- (16) Fernandez, C., Hattar, C. M., and Kerns, R. J. (2006) Semi-synthetic heparin derivatives: chemical modifications of heparin beyond chain length, sulfate substitution pattern and N-sulfo/N-acetyl groups. *Carbohydr. Res.* 341, 1253–1265.
- (17) Freudenberg, U., Hermann, A., Welzel, P. B., Stirl, K., Schwarz, S. C., Grimmer, M., Zieris, A., Panyanuwat, W., Zschoche, S., Meinhold, D., Storch, A., and Werner, C. (2009) A star-PEG-heparin hydrogel platform to aid cell replacement therapies for neurodegenerative diseases. *Biomaterials* 30, 5049–5060.
- (18) Tsurkan, M. V., Chwalek, K., Levental, K. R., Freudenberg, U., and Werner, C. (2010) Modular starPEG-heparin gels with bifunctional peptide linkers. *Macromol. Rapid Commun.* 31, 1529–1533.
- (19) Cui, F. Z., Tian, W. M., Hou, S. P., Xu, Q. Y., and Lee, I. S. (2006) Hyaluronic acid hydrogel immobilized with RGD peptides for brain tissue engineering. *J. Mater. Sci. Mater. Med.* 17, 1393–1401.
- (20) Maciag, T., Kadish, J., Wilkins, L., Stemerman, M. B., and Weinstein, R. (1982) Organizational behavior of human umbilical vein endothelial cells. *J. Cell Biol.* 94, 511–520.
- (21) Nie, T., Baldwin, A., Yamaguchi, N., and Kiick, K. L. (2007) Production of heparin-functionalized hydrogels for the development of responsive and controlled growth factor delivery systems. *J. Controlled Release* 122, 287–296.
- (22) Tsurkan, M. V., Chwalek, K., Prokoph, S., Zieris, A., Levental, K. R., Freudenberg, U., and Werner, C. (2013) Defined polymer-peptide conjugates to form cell-instructive starPEG-heparin matrices in situ. *Adv. Mater.* 25, 2606–2610.
- (23) Freudenberg, U., Sommer, J. U., Levental, K. R., Welzel, P. B., Zieris, A., Chwalek, K., Schneider, K., Prokoph, S., Prewitz, M., Dockhorn, R., and Werner, C. (2012) Using mean field theory to guide biofunctional materials design. *Adv. Funct. Mater.* 22, 1391–1398.
- (24) Mather, B. D., Viswanathan, K., Miller, K. M., and Long, T. E. (2006) Michael addition reactions in macromolecular design for emerging technologies. *Prog. Polym. Sci.* 31, 487–531.
- (25) Khan, A. T., Parvin, T., Gazi, S., and Choudhury, L. H. (2007) Bromodimethylsulfonium bromide mediated Michael addition of amines to electron deficient alkenes. *Tetrahedron Lett.* 48, 3805–3808.
- (26) Kalia, J., and Raines, R. T. (2007) Catalysis of imido group hydrolysis in a maleimide conjugate. *Bioorg. Med. Chem. Lett.* 17, 6286–6289.
- (27) Sapsford, K. E., Berti, L., and Medintz, I. L. (2006) Materials for fluorescence resonance energy transfer analysis: beyond traditional donor-acceptor combinations. *Angew. Chem., Int. Ed.* 45, 4562–4589.
- (28) Zieris, A., Prokoph, S., Levental, K. R., Welzel, P. B., Grimmer, M., Freudenberg, U., and Werner, C. (2010) FGF-2 and VEGF functionalization of starPEG-heparin hydrogels to modulate bio-molecular and physical cues of angiogenesis. *Biomaterials* 31, 7985–7994.
- (29) Massia, S. P., and Hubbell, J. A. (1991) An RGD spacing of 440 nm is sufficient for integrin alpha V beta 3-mediated fibroblast spreading and 140 nm for focal contact and stress fiber formation. *J. Cell Biol.* 114, 1089–1100.
- (30) Koo, L. Y., Irvine, D. J., Mayes, A. M., Lauffenburger, D. A., and Griffith, L. G. (2002) Co-regulation of cell adhesion by nanoscale RGD organization and mechanical stimulus. *J. Cell. Sci.* 115, 1423–1433.
- (31) Hirano, Y., Okuno, M., Hayashi, T., Goto, K., and Nakajima, A. (1993) Cell-attachment activities of surface immobilized oligopeptides RGD, RGDS, RGDV, RGDT, and YIGSR toward five cell lines. *J. Biomater. Sci., Polym. Ed.* 4, 235–243.
- (32) Pierschbacher, M. D., and Ruoslahti, E. (1987) Influence of stereochemistry of the sequence Arg-Gly-Asp-Xaa on binding specificity in cell adhesion. *J. Biol. Chem.* 262, 17294–17298.
- (33) Delforge, D., Gillon, B., Art, M., Dewelle, J., Raes, M., and Remacle, J. (1998) Design of a synthetic adhesion protein by grafting RGD tailed cyclic peptides on bovine serum albumin. *Lett. Pept. Sci.* 5, 87–91.
- (34) Chwalek, K., Levental, K. R., Tsurkan, M. V., Zieris, A., Freudenberg, U., and Werner, C. (2011) Two-tier hydrogel degradation to boost endothelial cell morphogenesis. *Biomaterials* 32, 9649–9657.
- (35) Ingber, D. E., and Folkman, J. (1989) How does extracellular matrix control capillary morphogenesis? *Cell* 58, 803–805.
- (36) Engler, A., Bacakova, L., Newman, C., Hategan, A., Griffin, M., and Discher, D. (2004) Substrate compliance versus ligand density in cell on gel responses. *Biophys. J.* 86, 617–628.
- (37) Gobin, A. S., and West, J. L. (2002) Cell migration through defined, synthetic ECM analogs. *FASEB J.* 16, 751–753.
- (38) Folkman, J., Haudenschild, C. C., and Zetter, B. R. (1979) Long-term culture of capillary endothelial cells. *Proc. Natl. Acad. Sci. U. S. A.* 76, 5217–5221.
- (39) Weis, J. R., Sun, B., and Rodgers, G. M. (1991) Improved method of human umbilical arterial endothelial cell culture. *Thromb. Res.* 61, 171–173.
- (40) De Bartolo, L., Morelli, S., Lopez, L. C., Giorno, L., Campana, C., Salerno, S., Rende, M., Favia, P., Detomaso, L., Gristina, R., d'Agostino, R., and Drioli, E. (2005) Biotransformation and liver-specific functions of human hepatocytes in culture on RGD-immobilized plasma-processed membranes. *Biomaterials* 26, 4432–4441.



- (41) Andersen, T., Strand, B. L., Formo, K., Alsberg, E., and Christensen, B. E. (2012) Alginates as biomaterials in tissue engineering. *Carbohydr. Chem.* 37, 227–258.
- (42) Park, K. M., Lee, S. Y., Joung, Y. K., Na, J. S., Lee, M. C., and Park, K. D. (2008) RGD-conjugated chitosan-pluronic hydrogels as a cell supported scaffold for articular cartilage regeneration. *Macromol. Res.* 16, 517–523.
- (43) Welzel, P. B., Prokoph, S., Zieris, A., Grimmer, M., Zschoche, S., Freudenberg, U., and Werner, C. (2011) Modulating biofunctional starPEG heparin hydrogels by varying size and ratio of the constituents. *Polymers* 3, 602–620.